Plasma Physics and Controlled Fusion

Sheared flows and turbulence in fusion plasmas

To cite this article: M A Pedrosa *et al* 2007 *Plasma Phys. Control. Fusion* **49** B303

IOP Publishing Plasma Physics and Controlled Fusion

Plasma Phys. Control. Fusion **49** (2007) B303–B311 doi:10.1088/0741-3335/49/12B/S28

Sheared flows and turbulence in fusion plasmas

M A Pedrosa[1], B A Carreras[1], C Hidalgo[1], C Silva[2], M Hron[3], L García[4], J A Alonso[1], I Calvo[1], J L de Pablos[1], J Stöckel[3]

[1] Laboratorio Nacional de Fusión, Asociación EURATOM/CIEMAT, 28040-Madrid, Spain
[2] Centro de Fusão Nuclear, Instituto Superior Técnico, Associaçao EURATOM/IST, 1049-001-Lisbon, Portugal
[3] Institute of Plasma Physics, Association EURATOM/IPP.CR, AS CR Prague, Czech Republic
[4] Universidad Carlos III, 28911-Leganés, Madrid, Spain

Received 6 July 2007
Published 16 November 2007
Online at stacks.iop.org/PPCF/49/B303

Abstract

The universality of the observed characteristics of sheared flows points to a general ingredient to explain the damping/driving mechanisms responsible for the development of these flows in the plasma boundary region of fusion devices. Experiments in the TJ-II stellarator showing that the generation of spontaneous sheared flows at the plasma edge requires a minimum plasma density or density gradient, open a unique possibility to characterize the dynamics of sheared flow development in fusion plasmas.

The effective viscosity at the plasma edge can be deduced by means of the decay rate of the perpendicular flow measurement once the driving force has been removed. Changes in the plasma rotation and turbulence have been studied when an electric field is externally applied at the plasma edge. The relaxation of flows and radial electric fields has been compared in the edge plasma region of TJ-II stellarator and CASTOR tokamak showing a striking similarity. The findings can help to test neoclassical and anomalous damping mechanisms in fusion plasmas.

Finally, the emergence of the plasma edge sheared flow as a function of plasma density can be explained using a simple second-order phase transition model that reproduces many of the features of the TJ-II experimental data while capturing the qualitative features of the transition near the critical point.

(Some figures in this article are in colour only in the electronic version)

1. Introduction

The importance of the shear in flows as a stabilizing mechanism to control plasma fluctuations in magnetically confined plasmas is well known [1]. In fact, it has been clearly established that $E \times B$ shear stabilization mechanisms are important for the improvement of plasma confinement in fusion devices. In particular both H-mode and core transport barriers are related to a large increase in the $E \times B$ sheared flow. As a consequence plasma flows play a crucial role on magnetically confined plasmas transport [1–3] and clarifying the driving/damping mechanisms of sheared flow is a key issue for the development of fusion. Both neoclassical (e.g. ion orbit losses [4]) and anomalous mechanisms (i.e. anomalous stringer spin-up [5] and Reynolds stress [6, 7]) have been considered as candidates to explain the generation of sheared flows. Atomic physics via charge-exchange momentum losses [8, 9], parallel viscosity (magnetic pumping) [10] and turbulent viscosity are considered as candidates to explain perpendicular flow damping physics. The role of neoclassical mechanisms to explain poloidal flows is an open issue in the fusion community [11–13].

This paper describes the generation of spontaneous edge sheared flows in the TJ-II stellarator and the relaxation flows and electric fields in the edge of the TJ-II stellarator and the CASTOR tokamak. The result of the experiments carried out in the TJ-II stellarator and the CASTOR tokamak [14] can help to understand and quantify the importance of anomalous versus neoclassical mechanisms on the damping physics of radial electric fields and flows in fusion plasmas.

The paper is organized as follows. In section 2 the experimental used set-up is presented; in section 3 the results of the spontaneous development of the shear flow in TJ-II are summarized. Section 4 describes the results on the time decay of the flow in TJ-II and CASTOR. The model coupling the shear flow and turbulence and the comparison with the experimental results is shown in section 5 and finally in section 6 the conclusions of the paper are presented.

2. Experimental set-up

Experiments were carried out in electron cyclotron resonance heated plasmas ($P_{\mathrm{ECRH}} = 200$–$400\,\mathrm{kW}$, $B_{\mathrm{T}} = 1\,\mathrm{T}$, $R = 1.5\,\mathrm{m}$, $\langle a\rangle \leqslant 0.22\,\mathrm{m}$, $\iota(a)/2\pi \approx 1.7$–$1.8$) obtained in the TJ-II stellarator. The plasma density was modified in the range $(0.35–1) \times 10^{19}\,\mathrm{m}^{-3}$. Different edge plasma parameters were characterized using a multi-Langmuir probe system, installed on a fast reciprocating drive (approximately $1\,\mathrm{m\,s}^{-1}$) that allows one to obtain radial profiles in a single shot [15].

A carbon composite mushroom-shaped electrode (12 mm high with a diameter of 25 mm) was developed and installed on another fast reciprocating drive equal to the one used with probes. The electrode was inserted typically 2 cm inside the last-closed flux surface (LCFS) and biased positively (200–300 V) with respect to one of the two poloidal limiters located in the scrape-off layer region (SOL) (about 0.5 cm beyond the LCFS). Measured electrode currents were in the range 30–50 A [16].

A Princeton Scientific Instruments intensified camera with a CCD sensor (PSI-5) with H_α filter, recording up to 250.000 frames per second, 64×64 pixels resolution and 1.2 ms total recording time at maximum speed was also used [17] to investigate the 2D structure of fluctuations during the shear flow development.

In the CASTOR tokamak ($R = 0.4\,\mathrm{m}$, $a = 85\,\mathrm{mm}$, $B_{\mathrm{T}} = 1\,\mathrm{T}$, $I_{\mathrm{p}} \approx 9\,\mathrm{kA}$, $q_{\mathrm{a}} \approx 10$), the poloidal rotation and plasma potential have been also modified by means of electrode biasing in the plasma edge region [18]. The electrode, located in the vicinity of the LCFS, at $r = 65$–$75\,\mathrm{mm}$ ($r/a \approx 0.75$–0.9), was biased ($U_{\mathrm{B}} = -400 - 250\,\mathrm{V}$) with respect to the vacuum vessel. Typical radial currents drawn by the electrode were up to about 30–40 A. Edge density and electron temperature were in the range of $n_{\mathrm{e}} \approx 1 \times 10^{12}\,\mathrm{cm}^{-3}$ and $T_{\mathrm{e}} \approx 10$–$20\,\mathrm{eV}$, respectively. Langmuir probes were used in the potential and flow measurements presented in this paper. The floating potential profile was measured using a rake probe with 16 single Langmuir probe tips that are radially separated by 2.54 mm, covering both the SOL and edge plasma regions ($r = 65$–$95\,\mathrm{mm}$). Further, a Mach probe of Gundestrup type was used for ion flows measurements [19].

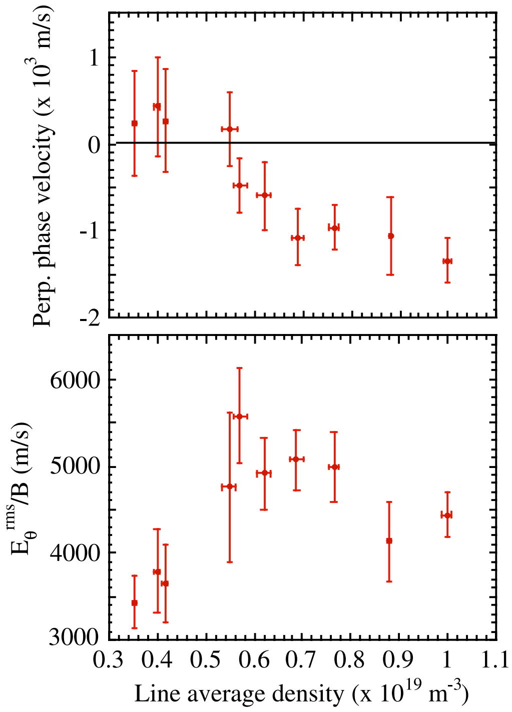

Figure 1. Perpendicular flows and the fluctuations of the perpendicular electric field from shot to shot measurements at different plasma density obtained at the TJ-II plasma edge ($r/a \approx 0.8$).

3. On the spontaneous development of the shear flow in TJ-II

It has been previously shown that the development of the sheared flows at the plasma edge of the TJ-II requires a critical value of the plasma density or density gradient [20,21] that depends on the plasma magnetic configuration [22].

The experiments in TJ-II have been performed using different set-ups for changing density and a remarkable reproducibility of the results has been obtained for the different approaches as is described in detail in [21]. As a summary, figure 1 shows the perpendicular flows and the fluctuations of the perpendicular electric field (i.e. the turbulent radial velocity $\tilde{v}_r = \tilde{E}_\theta/B$) deduced from measurements at the plasma edge of the TJ-II ($r/a \approx 0.8$, where a is the averaged minor radius of the plasma), obtained changing density from shot to shot. As plasma density increases shear flow develops, and considerable changes in the radial profiles of edge magnitudes were observed [20,21]. Consistent with the changes in the floating potential, above a threshold density value ($\approx (0.5$–$0.6) \times 10^{19}\,\mathrm{m}^{-3}$ for the configuration shown in figure 1) the perpendicular phase velocity reverses sign at the plasma edge from positive to negative values due to the development of the natural shear layer, with a shearing rate of about $10^5\,\mathrm{s}^{-1}$ of the order of the inverse of the correlation time of fluctuations ($\mathrm{d}v_\theta/\mathrm{d}r \approx 1/\tau \approx 10^5\,\mathrm{s}^{-1}$) [23]. Below the critical density, the edge shear layer, which has been observed in the proximity of the LCFS in all magnetic confinement devices verifying $\mathrm{d}v_\theta/\mathrm{d}r \approx 1/\tau$, does not exist in TJ-II, at least up to 3 cm inside the LCFS ($r/a \approx 0.8$) where the innermost measurements have been obtained. It is important to note that the levels of turbulent transport and fluctuations increase as density increases up to the critical value for which sheared flow is developed. Beyond this

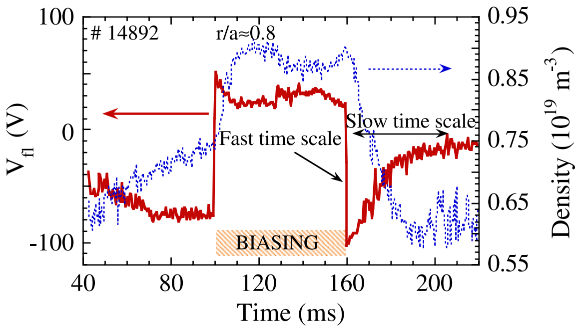

Figure 2. Time scales of floating potential signal evolution measured inside the LCFS ($r/a \approx 0.8$) in TJ-II. Slow time scale evolves as the line average plasma density.

point, fluctuations and turbulent transport slightly decrease although edge gradients become steeper.

Fast imaging of the plasma edge in shots with different values of density revealed an effect of the shear layer on turbulent structures [24].

4. Relaxation time scales measurements in TJ-II and CASTOR

The modifications in the plasma properties induced by electrode biasing depend on several parameters such as the biasing voltage, the electrode location and the plasma density. The latter is very important on TJ-II as the edge parameters and global plasma confinement depend strongly on it [20, 21]. The response of the plasma to bias is, therefore, different at densities below and above the threshold value to trigger the spontaneous development of $E \times B$ sheared flows [16]. The results of the TJ-II biasing experiments presented in this paper correspond to positive applied bias in the plasma edge of TJ-II. The changes observed in the edge profiles, edge electric fields and fluctuation levels show evidence of biasing induced improved confinement as was observed in previous limiter biasing experiments in TJ-II [25].

The floating potential profile is strongly modified by the electrode bias in the region $r/a < 0.9$, leading to the formation of a strong positive radial electric field (up to $10\,\mathrm{kV\,m^{-1}}$). These are consistent with the observed changes of the perpendicular phase velocity due to the $E \times B$ drift. Similar electrode bias response has been reported in CASTOR tokamak: floating potential and radial electric field profiles are significantly modified at both sides of the electrode location [26].

As in the spontaneous development of the shear [27], two different time scales arise in the relaxation of externally induced electric fields in TJ-II: a slow time scale, in the range of the particle confinement time (tens of milliseconds) that evolves with plasma density, and a fast time scale in the range of few turbulence correlation times. Figure 2 shows the two time evolution scales of the floating potential signal measured inside the LCFS ($r/a \approx 0.8$) in TJ-II together with the evolution of plasma density with biasing.

The fast time evolution of floating potential signals (V_{fl}), when biasing is switched off, can be fitted to an exponential function using the expression

$$V_{fl}(t) = V_{max}\exp(-t/\tau) + V_{min} \qquad (1)$$

from which the exponential relaxation time τ is deduced (see figure 3(*b*)). This fitting procedure has been done for floating potential signals measured at different densities and at different radial locations.

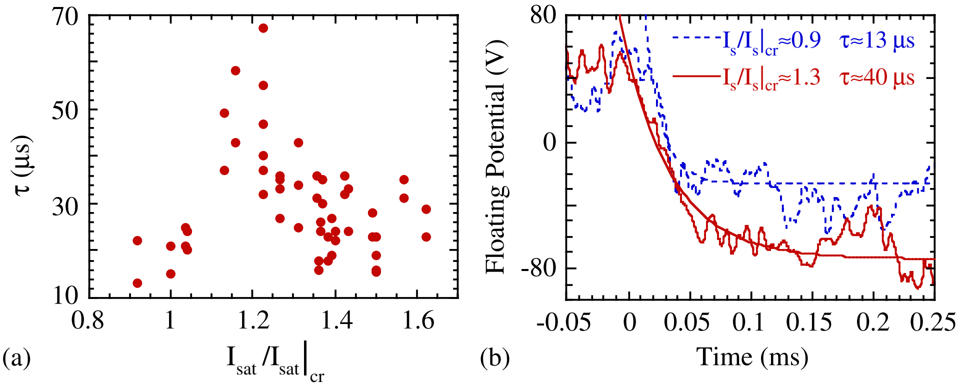

Figure 3. (*a*) Behaviour of the measured relaxation time at the TJ-II plasma edge ($0.75 < r/a < 0.85$) as a function of normalized ion saturation current after switch-off the biasing and (*b*) the corresponding signals and fitting for two different values of the control parameter.

Experimental results show that the fast time decay of the floating potential signals after switching off the biasing can be fitted by an exponential decay with characteristic time decay in the range 10–100 μs.

The influence of plasma density (in the range $(0.4\text{–}1) \times 10^{19}\,\mathrm{m}^{-3}$) on relaxation times has also been investigated in TJ-II. In order to compare with results obtained from the model as is presented in the next section, and to use a more realistic control parameter (i.e. the local density gradient) the average ion saturation current, measured when switching off the biasing and normalized to its value at the critical point (i.e. when shear flow develops) has been used. Figure 3 shows the behaviour of the measured relaxation time at the TJ-II plasma edge ($0.75 < r/a < 0.85$) after switch-off of the biasing as a function of the above mentioned control parameter as well as the corresponding signals and fits for two different values of the parameter. Results suggest an increase in decay times above the critical value of the control parameter (i.e. once edge perpendicular sheared flows are fully developed).

The fast transients described have been also assessed with the fast camera. Results of the characteristic times and velocities of the observed moving blobs are in good agreement with probe results [24].

As in TJ-II, the radial profiles of the floating potential measured in the plasma edge region of the CASTOR tokamak [26] are strongly modified by biasing. Relaxation times of both plasma floating potential and plasma rotation have been investigated after the electrode bias switch-off. The characteristic relaxation time has been determined from the time evolution of floating potential signals with the same fitting function than in TJ-II (equation (1)). The time decay and the fitting of the floating potential signals have been obtained at different plasma radius. The results are in the range 10–30 μs (figure 4).

Table 1 shows a summary of the parameters and the experimental results in the devices under comparison in this work. Present investigations show that the experimentally measured damping time of plasma potential is in the range 10–70 μs, independently of the type of device. Similar results have been reported in the HSX stellarator [28, 29].

Poloidal flows can be damped by parallel viscosity (magnetic pumping) [30]. In the plateau/collisional regime, the poloidal momentum damping time has been estimated for CASTOR edge plasma parameters in the range of some hundreds of μs.

Turbulence is also an important element in the physics of flows and electric fields. Turbulent damping mechanisms are likely to apply for short time scales, in the order of few

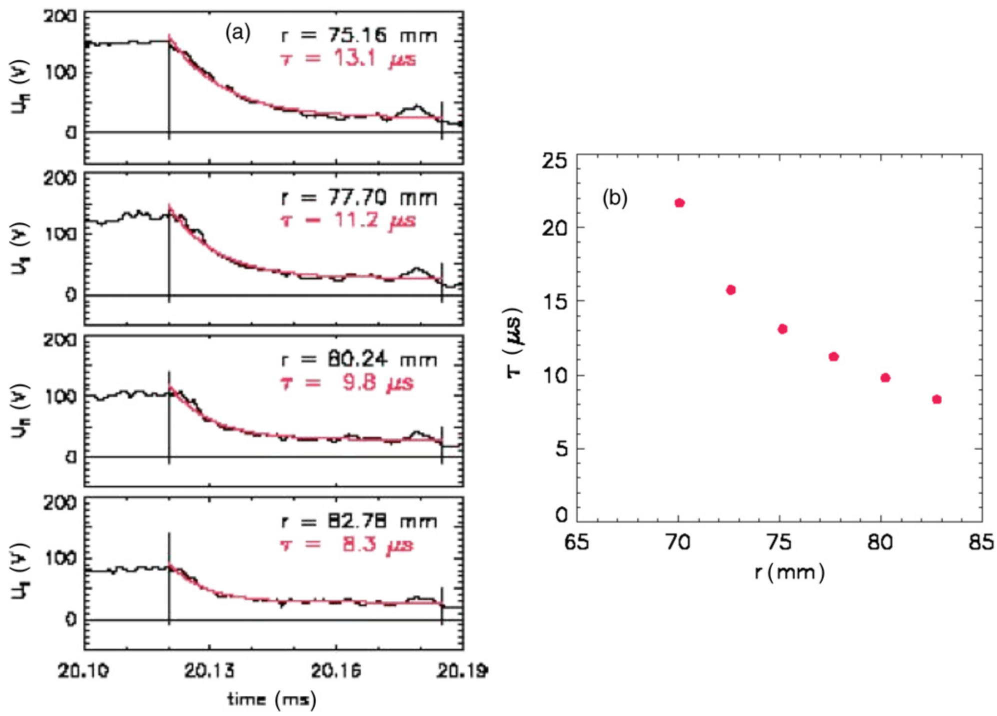

Figure 4. (*a*) Fit (red lines) of the floating potentials decay measured at different plasma radius of CASTOR tokamak and (*b*) behaviour of the decay time as a function of radius. The electrode is located at $r = 75$ mm.

Table 1. Summary of parameters of studied devices.

Device	TJ-II Stellarator	CASTOR Tokamak
Major radius (m)	1.5	0.4
Magnetic field (T)	1	1
Line average density (m^{-3})	$(0.4–1) \times 10^{19}$	1×10^{18}
Relaxation time (μs)	10–70	10–30

turbulence correlation times (typically $\tau_c \approx 10\,\mu$s), this being consistent with experimental time decay findings. Momentum loss via atomic physics mechanisms (charge exchange) might also play a role. However, using typical plasma edge parameters damping times due to charge exchange are expected to be of the order of hundred of μs, this being significantly larger than the experimental decay measurements.

5. Model coupling shear flow and turbulence and comparison with experimental results

In the mid-1990s, a simple model [31] was proposed to explain the transition from low (L-mode) to high confinement mode (H-mode) [32]. The model consists of a coupled envelope equations for the fluctuation intensity and the mean electric field shear. In the model the transition appears as a second-order phase transition with the order parameter the poloidal velocity shear V'_θ. The mechanism for the transition is a flow shear dynamo instability that amplifies the shear flow through the Reynolds stress term. The amplified sheared flow reduces the turbulence fluctuations through the associated sheared electric field turbulence suppression effect [1,33].

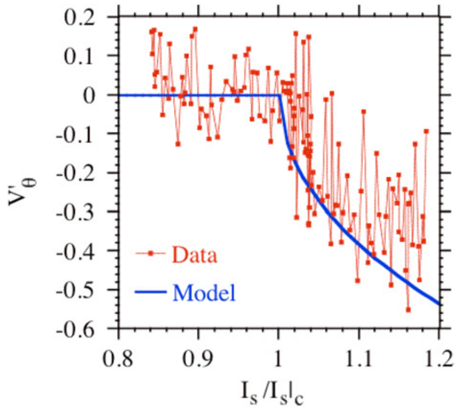

Figure 5. Comparison between the velocity shear obtained by the model and from the experimental data.

A later extension of this model [34] incorporated the diamagnetic terms. Therefore the sheared electric field now resulted from the combination of the sheared poloidal flow and the pressure gradient. This model, as the pressure increases, predicts two successive transitions. The first one is a second-order phase transition controlled by the poloidal shear flow and leads to a reduction of the turbulence level. The second is a first-order phase transition controlled by the pressure gradient that leads to the suppression of turbulence. This second state seems to describe well the H-mode state.

The first transition (the second-order one) is essentially the same one given by the initial model and has the characteristic properties of the emergence of the sheared flow layer. We have used the transition model to compare the predictions of this first transition with the experimental results of the formation of this sheared flow layer, as observed in TJ-II. In order to do so, we normalize all the physical magnitudes to their values at the critical point so we can write the solutions of the model in terms of measurable quantities [35].

Figure 5 shows a comparison between the velocity shear obtained by the model and deduced from the experimental data as a function of the control parameter defined from the ion saturation current as explained above. Comparisons between the model and experimental data show that in spite of the simplicity of the model, it captures the qualitative features of the transition near the critical point. Note that the model has no free parameters once the position of the critical point is determined. Of course this comparison does not confirm the exact values of the power dependences, but it shows that they are compatible with the data. We have considered plasmas with more complicated density evolutions that a simple ramp and results are also in good agreement with experiments [35].

In spite of the difficulty of interpreting the decay rate in terms of viscosity, an effective viscosity at the plasma edge can be determined by measuring the decay rate of the perpendicular flow once the driving force has been removed. A biased electrode can produce this driving force externally. Decay rate times obtained from biasing experiments performed in TJ-II (see section 4) have been used as input to investigate the properties of the damping rate in the framework of a model based in the one previously described with the addition of an external drive. Looking at short time scales after switching off the bias potential, the model reproduces the exponential decay of the flow and also shows an increase in the decay time close to the critical point (figure 6), giving a qualitative description of the change in the decay time obtained experimentally that has been shown in figure 3(*a*).

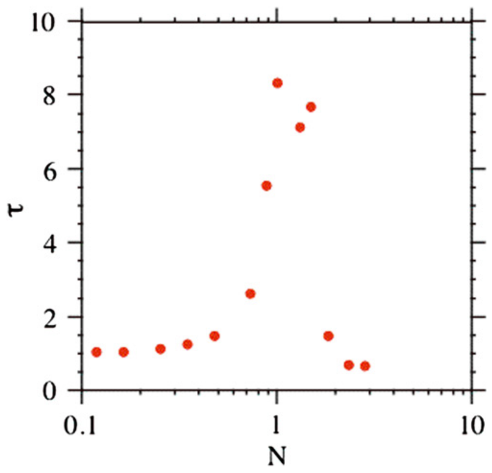

Figure 6. Decay time obtained by the model as a function of the local average ion saturation current normalized at the corresponding critical point (development of shear flow).

6. Conclusions

- The development of the naturally occurring velocity shear layer in TJ-II requires a minimum plasma density/gradient that depends on the magnetic configuration and plasma volume. Sheared flows appear to be organized near marginal stability with fluctuations in TJ-II. The universality of this property is easily understood assuming that edge sheared flows are controlled by turbulence. Results have a direct impact in the understanding of the physics responsible for the generation of critical sheared flows, pointing to the important role of turbulence as a driving mechanism.
- Two time scales have been found for edge plasma potential decay measured in the TJ-II edge plasma region when electrode applied potential is turned off. In the fast time scale (10–70 μs) the plasma potential changes in the edge region by about 50–100 V after biasing; in the slow time scale (comparable to the particle confinement time) plasma potential modifications are linked to the evolution of the plasma density.
- Measurements of the fast decay time in the TJ-II stellarator suggest an increase in decay times above the threshold gradient value to trigger the emergence of shear flow (i.e. once edge perpendicular sheared flows are fully developed).
- The similarity between decay time scales measured in TJ-II and CASTOR, being devices with different values of ripple (and consequently neoclassical viscosity), and the fact that measured fast decay times are in the range of few turbulence correlation times, suggests the important effect of anomalous (turbulent) mechanisms in the damping rate of sheared flows in the plasma boundary of fusion devices.
- The emergence of the plasma edge shear flow as a function of the plasma density can be explained using a simple second-order phase transition model. This simple model reproduces many of the features of the TJ-II experimental data and shows that in spite of the simplicity of the model, it captures the qualitative features of the transition near the critical point.

Acknowledgments

The authors would like to thank V Tribaldos, K McCarthy and M A Ochando for helpful discussions. We would also like to acknowledge support from the technicians, the data acquisition group and the whole TJ-II team.

This research was sponsored in part by Ministerio de Educación y Ciencia of Spain under Projects ENE2006-15244-C03-01 and ENE2006-15244-C03-02.

References

[1] Terry P W 2000 *Rev. Mod. Phys.* **72** 109
[2] Burrel K 1999 *Phys. Plasmas* **6** 4418
[3] Carreras B A 1997 *IEEE Trans. Plasma Sci.* **25** 1281
[4] Shaing K C and Crume E C 1989 *Phys. Rev. Lett.* **63** 2369
[5] Hassam A B and Antonsen T M 1994 *Phys. Plasmas* **1** 337
[6] Diamond P H and Kim Y B 1991 *Phys. Fluids* **3** 1626
[7] Carreras B A, Lynch V E and García L 1991 *Phys. Fluids* B **3** 1438
[8] Monier-Garbet P *et al* 1997 *Nucl. Fusion* **37** 403
[9] Mahdavi M A *et al* 1990 *J. Nucl. Mater.* **176–177** 32
[10] Hirsman S P 1987 *Nucl. Fusion* **18** 917
[11] Crombé K *et al* 2005 *Phys. Rev. Lett.* **95** 155003
[12] Solomon W M *et al* 2006 *Phys. Plasmas* **13** 056116
[13] Severo J H F *et al* 2003 *Nucl. Fusion* **43** 1047
[14] Pedrosa M A *et al* 2006 *Proc. 21st IAEA Conf. (Chengdu, China)*
[15] Pedrosa M A *et al* 1999 *Rev. Sci. Instrum.* **70** 415
[16] Silva C *et al* 2005 *Czech. J. Phys.* **55** 1589
[17] Alonso J A *et al* 2005 *Proc. 32nd EPS Conf. (Tarragona, Spain, 2005)*
[18] van Oost G *et al* 2001 *J. Plasma Fusion Res. Ser.* **4** 29
[19] Gunn J P *et al* 2001 *Czech. J. Phys.* **51** 1001
[20] Hidalgo C *et al* 2004 *Phys. Rev.* E **70** 067402
[21] Pedrosa M A *et al* 2005 *Plasma Phys. Control. Fusion* **47** 777
[22] Pedrosa M A *et al* 2005 *Czech. J. Phys.* **55** 1579
[23] Hidalgo C, Pedrosa M A and Gonçalves B 2002 *New J. Phys.* **4** 51.1
[24] Alonso J A *et al* 2006 *Plasma Phys. Control. Fusion* **48** B465
[25] Hidalgo C *et al* 2004 *Plasma Phys. Control. Fusion* **46** 287
[26] Hron M *et al* 2003 *Proc. 14th Int. Stellarators Workshop (Germany)*
[27] Gonçalves B *et al* 2006 *Phys. Rev. Lett.* **96** 145001
[28] Gerhardt S P *et al* 2005 *Phys. Rev. Lett.* **94** 015002
[29] Gerhardt S P *et al* 2005 *Phys. Plasmas* **12** 056116
[30] Hirshman S P 1978 *Nucl. Fusion* **18** 917
[31] Diamond P H, Liang Y M, Carreras B A and Terry P W 1994 *Phys. Rev. Lett.* **72** 2565
[32] Wagner F *et al* 1982 *Phys. Rev. Lett.* **49** 1408
[33] Biglari H, Diamond P H and Terry P W 1990 *Phys. Fluids* B **2** 1
[34] Carreras B A, Newman D E, Diamond P H and Liang Y-M 1994 *Phys. Plasmas* **1** 4014
[35] Carreras B A *et al* 2006 *Phys. Plasmas* **13** 122509